

Precast concrete wall-raft connectors for increasing the lateral load capacity: An experimental and analytical approach

P. SenthilKumar, D. Tensing, G. Hemalatha, S. Vivekananda Sharma, C. Daniel

Online Publication Date: 10 October 2023

URL: <http://www.jresm.org/archive/resm2023.762me050.html>

DOI: <http://dx.doi.org/10.17515/resm2023.762me050>

Journal Abbreviation: *Res. Eng. Struct. Mater.*

To cite this article

SenthilKumar P., Tensing D., Hemalatha G., Sharma SV, Daniel C. Compression strength behaviour of fibre-reinforced concrete made with hoop-shaped waste polyethylene terephthalate fibre. *Res. Eng. Struct. Mater.*, 2024; 10(1): 1-22.

Disclaimer

All the opinions and statements expressed in the papers are on the responsibility of author(s) and are not to be regarded as those of the journal of Research on Engineering Structures and Materials (RESM) organization or related parties. The publishers make no warranty, explicit or implied, or make any representation with respect to the contents of any article will be complete or accurate or up to date. The accuracy of any instructions, equations, or other information should be independently verified. The publisher and related parties shall not be liable for any loss, actions, claims, proceedings, demand or costs or damages whatsoever or howsoever caused arising directly or indirectly in connection with use of the information given in the journal or related means.



Published articles are freely available to users under the terms of Creative Commons Attribution - NonCommercial 4.0 International Public License, as currently displayed at [here](https://creativecommons.org/licenses/by-nc/4.0/) (the "CC BY - NC").

Precast concrete wall-raft connectors for increasing the lateral load capacity: An experimental and analytical approach

P. SenthilKumar^{1,a}, D. Tensing^{1,b}, G. Hemalatha^{1,c}, S. Vivekananda Sharma^{*,1,d}, C. Daniel²

¹Department of Civil Engineering, Karunya Institute of Technology and Sciences, India

²Department of Civil Engineering, Hindustan Institute of Technology and Science, India

Article Info

Abstract

Article history:

Received 08 May 2023

Accepted 07 Oct 2023

Keywords:

Precast;

Structural walls;

Rafts;

Lateral load;

Reinforced concrete;

Cyclic loading

Precast structural walls and rafts commonly resist lateral load in structures owing to improved traits and faster construction. The behavior of five different types of precast reinforced concrete structural wall and raft connection systems is evaluated in this study. In all five configurations, the cyclic load is applied in the wall systems to observe the lateral load-carrying capacity and hysteretic characteristics. The damage and failure patterns were assessed. To confirm and contrast the behavior of the proposed precast structural wall and raft connection systems with the experimental findings, FEM analysis was used. Only shear and flexural cracks were observed. The specimen with 12 mm dia rods has the maximum load carrying capacity of 10.23 kN in the negative cycle, which is 57% more than the specimen without grouting and connector. The suggested connection can improve the resistance behavior in all key directions by absorbing more energy than precast walls under dynamic load.

© 2024 MIM Research Group. All rights reserved.

1. Introduction

Precast concrete buildings are frequently used to construct structures in developed nations, particularly urbanized regions. Precast concrete structures are superior to traditional cast-in-place concrete structures in design and construction, including better structural components, faster construction, and lower noise. To protect the integrity of the structure of precast concrete buildings during lateral loads like wind or earthquakes, precast concrete structures in many countries have been restricted to buildings of less than ten stories. Arthi et al. conducted experimental research to examine the dowel connection's shear capacity under reverse cyclic loading. The investigation entailed comparing the findings of the real experiments with the numerical analysis of the dowel connection between the precast shear wall and slab. According to the study, the ultimate strength of the dowel connection in the push and pull directions of loading was 11.17 kN and 11.03 kN, respectively[1]. Arthi et al. employed ABAQUS to simulate a dowel connection between the precast shear wall and slab to examine joint failure, damage, and hysteresis. The studied specimen showed a failure pattern consistent with the "Strong joint-Weak member." The findings of the finite element analysis were 11% higher than the outcomes of the actual tests. Using scaled-down models that were one-third the size of the actual connection. According to the study, the precast specimen's ductility factor and cumulative ED were higher than those of the monolithic specimen by 128.95% and

*Corresponding author: bom03vivek@gmail.com

^a orcid.org/0000-0001-9871-9037; ^b orcid.org/0000-0001-7806-001X; ^c orcid.org/0000-0001-7067-3786;

^d orcid.org/0000-0003-4923-621X; ^e orcid.org/0000-0002-4024-4742

DOI: <http://dx.doi.org/10.17515/resm2023.762me0508>

Res. Eng. Struct. Mat. Vol. 10 Iss. 1 (2024) 1-22

74.34%, respectively [2,3]. The importance of connecting zones in structural systems, particularly in buildings situated in seismic zones, was emphasized by Bannan in his research. He conducted a study to determine how seismic load combinations affected the behaviour of slabs at the points connected to shear walls. The parts of reinforced concrete buildings where the slabs meet the walls are considered the most important [4]. Precast concrete shear walls with low reinforcing, frequently utilized in Dutch residential structures of intermediate height, were the focus of Brunesi's research. Push and pull tests on precast wall connections were also conducted following the asymmetric approach as part of the study, and the results were used to illustrate how these joint systems behave cyclically under the influence of simulated seismic loads. Brunesi tested a 2-story precast concrete wall-slab-wall structure with minimal reinforcement in the Groningen area, where recent seismic occurrences brought on by gas extraction reservoir depletion have occurred. This building was picked to symbolize a common type of house in the region. Brunesi studied five specimens' monotonic and cyclic response curves, and the resulting damage patterns showed that the reported flexural failure mechanism was extremely stable and closely matched that shown in full-scale building tests. A mock-up of a building was tested using a shake table by Brunesi, who ran it through five iterations of increasing test intensity. Steel connectors used to connect the longitudinal and transverse walls finally failed, causing the structure to collapse [5-8]. Using fibre-reinforced polymer (FRP), Chalot studied the mechanical performance of full-scale reinforced concrete (RC) wall-slab connections under cyclic loading. It was found that Composite reinforcement increased joint strength by 80% and ductility by 33%. Reinforcement changed the failure mode from wall bending to joint shear. The composite strengthening also led to a 385% increase in the joint's ability to dissipate energy by relocating the failure zone [9]. Devine performed 20 tests to examine the relationship between connections' capacity for horizontal shear and their vertical uplift. Findings from three specimens are given, including reverse cyclic shear with 50 mm uplift, monotonic uplift, and cyclic uplift. It was found that the existing welding procedure utilized to connect the steel angle embedded in the concrete slab to the plate installed in the wall caused the weld to fail after just a few uplift cycles. Devine also created a nonlinear analytical model for wall-to-slab connectors to provide nonlinear dynamic analysis for assessing deformation needs during extreme seismic events [10]. Guo tested the seismic performance of a revolutionary precast structural system using a shaking table on a scaled-down, three-story model. The system was discovered to have a high collapse margin ratio, rigidity, and load capacity. There were created fragility curves for both the structural and nonstructural elements [11]. Hamicha performed a nonlinear finite element analysis of a reinforced concrete external shear wall-slab connection subjected to cyclic loading using the ABAQUS software package. The study examined structural reactions, including load-bearing capability, Energy Dissipation, ductility, and stiffness deterioration. To assess their impact on the structural response of the connection, study characteristics included connection type, the aspect ratio of slab thickness to shear wall thickness, the aspect ratio of shear wall height to the effective width of the slab, and concrete strength [12]. According to Hemamalini, the connections are a crucial element in the precast wall system's ability to resist lateral loads because they are the weakest point. The most significant difficulty is the connections' behaviour and potential failure when subjected to intense lateral loads and natural hazards. The article briefly examines shear walls' horizontal and vertical connections and their performance under various loading patterns [13]. Henry's study uses a wall-to-floor connection for a rigid cast-in-place connection to protect the floor from serious damage. This method isolates the floor from the vertical displacement and rotation of the wall. Rocking walls are only one effect of the wall-to-floor contact on a building's seismic response. It can be much more crucial for typical reinforced concrete walls, increasing their vulnerability to shear or axial failure [14]. The construction of computational models to validate the stress levels of structural components was made possible by Krentowski's assessment of the physical and

mechanical characteristics of the materials used to make connections. A suggestion for effectively strengthening weak connections was developed based on the research, computations, and analyses. Also, suggestions for efficient interlayer connection testing methods for challenging interlayer connections were suggested [15]. Lu created a novel structural method for precast concrete wall panels that connects using bolts for low-rise structures in rural areas. The ground-breaking technique enables dispersed bolt connections between permanent foundation walls, floors, and connecting columns. This capability makes it possible to disassemble and rebuild the complete system as necessary. However, the bolted joints displayed an unfavourable punching shear failure, as they could not exploit the strength of the wall panels completely, according to the findings of the prior quasi-static cycle push-over test [16]. Pavel examined Bucharest's 12-story reinforced concrete structure's seismic performance. Many new city office buildings use a flat slab supported by columns and strong, reinforced concrete core walls [17]. Through a significant experimental effort, Pavese investigated the behaviour of prefabricated reinforced concrete sandwich panels (RCSPs) under simulated seismic loading. Full-scale panels were used in tests to simulate the behaviour of fixed-end and cantilever walls that resist lateral forces. Moreover, tests were performed on a two-story, full-scale H-shaped structure of individually linked panels [18]. Rossley's study concentrated on using loop bars to connect precast concrete walls on the exterior and inside of a building. A transverse bar is inserted to guarantee continuity between the looping bars, resulting in a gap between the walls filled with concrete to create a firm connection. Analyzing the behaviour of the loop bar connection under shear force was the main goal of the experimental inquiry. [19] Shen proposed using slotted floor slabs, which have spaces close to the wall limbs and are filled with polystyrene, to improve the independent deformation of the limbs. The study's primary goal was to understand better how the limbs of shear walls and slotted floors interact. Three reinforced concrete prefabricated shear wall samples with shear keys were created to accomplish this. The study discovered that by adding slots to the floor slabs, concentrated deformation could be eased, and the slabs would be better protected. Shen conducted an experimental investigation to examine how a novel connection between walls and slabs that used high-performance concrete (HPC) post-casted in the core region responded to a fire. For comparison, three full-scale specimens—two completed connections and one cast-in-place connection underwent monotonic static loading testing before and after the fire [20-21]. The efficacy and durability of connections between precast panel joints are essential considerations, according to Singhal's study on the seismic behaviour of precast buildings. The total seismic performance of precast structures is significantly influenced by the transmission of loads and the ductility of the joint connections. Correct connection design is also required to transmit seismic forces between the precast panels effectively.

Singhal researched the seismic behaviour of a cast-in-place concrete hollow core precast reinforced concrete shear wall. The wall was under lateral stress and assessed for seismic characteristics, damage patterns, and lateral load capacity. Because of its ductile reaction, the wall demonstrated competent deformation properties. Precast RC wall connections, codal provisions, a study of experimental results, and the impact of post-tensioning on precast RC walls were all reviewed by Singhal. The precast wall-column system and the precast double-leaf system are two different kinds of precast reinforced concrete structural wall systems whose performance is evaluated by Singhal. The former uses loop bars to connect a precast wall to precast hollow columns, while the latter uses two precast panels with an in-situ concrete-filled hollow core. The hysteretic characteristics that resulted from applying lateral loads to both wall systems in a displacement-controlled cyclic mode were carefully evaluated regarding the damage pattern and numerous seismic properties. Singhal looked at the seismic behaviour of a full-scale precast reinforced

concrete wall exposed to in-plane cyclic loading and out-of-plane loading simulated by sand backfill.

The tested wall showed substantial out-of-plane movement and flexural fractures because of the high aspect ratio and lateral pressure from the backfill [22-26]. Tatsambon's study concentrated on the connections between slabs and walls because these components are frequently extended to the connection axis, assuming complete rotation [27]. Vaghei proposed a novel method for joining two adjacent precast wall panels utilizing two steel U-shaped channels. To provide a solid connection, these channels are fastened to the sides of the walls and joined together as male and female joints using bolts and nuts. A U-shaped rubber piece is fitted between the two channels to reduce any vibration impact within the structure. Vaghei looked into how well a precast concrete structure with a novel connection performed. The study concentrated explicitly on connections between precast concrete panels in industrial structures that used a unique U-shaped steel channel connector. The examination covered crack propagation, plastic strain trends in the concrete panels and connections, the primary stress distribution, and deformation of concrete panels and welded wire mesh reinforcements (BRC) [28-29]

Wang suggested the concept of equivalent cross-sectional area, in which the flexural strength of the horizontal part of the interior wall-slab joints is estimated using a coefficient known as the equivalent cross-sectional area ratio. These joints are essential in constructions with strong walls and thick slabs [30]. According to Xia, the precast specimens showed a flexural collapse at the end of the beam with no severe damage to the joint or shear wall. The four specimens' hysteresis curves revealed a pinching behaviour. The energy dissipation capacities of the precast specimens were on par with those of the cast-in-place specimens [31]. Three samples of precast slabs and monolithic walls subjected to quasi-static loads were compared in a study by Zenunovic. Mathematical models were created using displacement and FEM techniques to examine the connection types of both specimens. The stiffness matrix was modified by adding a semi-rigid parameter to the connection. [32]

The current investigation examines the wall-raft connectors' performance in precast structural elements under cyclic loading conditions. The specimens are designed and modelled using six different configurations in the Ansys tool for numerical simulation. The results obtained from the simulation are then validated through experimental investigation, with a focus on load-carrying capacity and energy dissipation. There are six configurations to consider in this study. These configurations include i) a wall raft without a connector and no grouting, ii) a wall raft without a connector but with grouting, iii) a wall raft with a shear connector of 8mm, iv) a wall raft with a shear connector of 10mm, v) a wall-raft with a shear connector of 12mm, and vi) a wall-raft with a shear connector of 12mm subjected to earthquake loading.

2. Simulation of Pre-Cast Model Using Finite Element Analysis (FEA)

Modeling is one of the important features in Finite Element Analysis. It takes around 40% to 60% of the total solution time. Improper modeling of the structures leads to the unexpected errors in the solution. Hence, proper care should be taken for modeling the structures. A good idealization of the geometry reduces the running time of the solution. The raft and wall are modelled using ANSYS software, considerably. In many situations, a three dimensional structure can easily be analyzed by considering it as a two dimensional structure without any loss of accuracy. Creative thinking in idealizing and meshing of the structure helps not only in reducing considerable amount of time but also in reducing the memory requirement of the system. Flow plasticity theory has been widely used for nonlinear simulation of RC structures. Constitutive reactions of flow plastic theory

in CAE software are referred to as material model. In the current modelling Menetrey-William model is used. The Menetrey-William constitutive model can well capture important mechanical behaviours of concrete such as tensile strength, compressive strength, nonlinear hardening, softening and dilatancy.

Finite Element modeling of Raft and wall assembly in ANSYS consist of three stages, which are listed as (a) Selection of element type (b) Assigning material properties (C) Modeling and meshing the geometry

Table 1. Details of Element and material properties

S.No	Name	Material	ANSYS Element
1	Concrete	M20	SOLID 185
2.	Steel Reinforcement	Fe550	BEAM 188
3.	Connecting rod	Fe550	BEAM 188

To create the finite element model in ANSYS WORKBENCH 2022 there are multiple tasks that have to be completed for the model to run properly for this model, ANSYS DESIGN MODELER environment was utilized to create the model the reinforcement (1D model) using concept tool and concrete model (3D model) by using extrude tool as shown in the figure below. Properties of concrete and reinforcements used in the development of model is presented in Table 1 and Table 2 respectively.

Table 2. Details of concrete element

Property	Values	Property	Values
Young's Modulus	31623N/mm ²	Plastic strain at uniaxial compressive strength	0.001
Poisson's ratio	0.15	Plastic strain at transition from power law to exponential softening	0.002
Bulk Modulus	1.5x10 ⁵ N/mm ²	Relative stress at start of nonlinear hardening	0.33
Shear Modulus	1.37x10 ⁵ N/mm ²	Residual relative stress at transition from power law to exponential softening	0.85
Uniaxial Compressive strength	20N/mm ²	Residual compressive stress	0.2
Uniaxial tensile strength	2.2	Mode 1 area specific fracture energy	50
Biaxial Compressive strength	25	Residual tensile relative stress	0.1
Dilatancy Angle	30		

Table 3. Details of steel element

Property	Values
Density	7850 kg/m ³
Young's Modulus	2x10 ¹¹ N/mm ²
Poisson's ratio	0.3
Bulk Modulus	1.66x10 ⁵ N/mm ²
Shear Modulus	7.69x10 ⁴ N/mm ²
Yield Strength	550 N/mm ²
Tangent Modulus	0

As per the designed scaled model, the wall and raft are modelled separately with reinforcement, as shown in Figure 1 and the assemble model with and without connector rod is shown in Figure2.

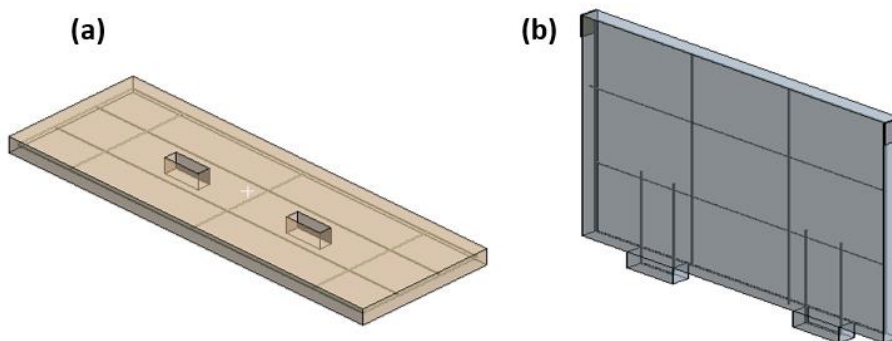


Fig. 1 Modelling of a) Raft b) Wall

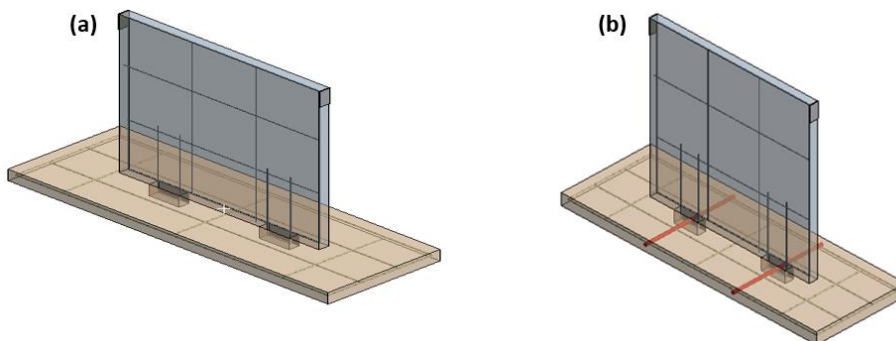


Fig. 2 Assembly of Raft and Wall a) with connector, b) without connector

The FEA of the raft and wall connection is carried out in ANSYS software. The material properties and meshing fineness was generated appropriately, for shell elements of 10 mm size were used for meshing. In the precast raft and wall connection study, five different configurations are studied, namely i) without connector, ii) with grouting, iii) raft and wall connection with 8 mm rod, iv) raft and wall connection with 10 mm rod v) raft and wall

connection with 12 mm rod. The specimens' models have been elaborated per IS 456:2021. ANSYS was employed to model and examine the specimens to confirm the experimental test results. The modelling tool highlights the specimen's meshing and the rod in red, as shown in Figure 3. The model needs boundary conditions for restriction to have a unique solution. Boundary conditions must be imposed on the faces to guarantee that the model performs similarly to the experiment. The bottom of the raft is fully constrained in all DOF, and reverse cyclic loading in the displacement-controlled method is applied on the top face of the wall. The maximum deflection occurs at 37.94 mm. The simulated raft and wall connection without connection is shown in Figure 4.

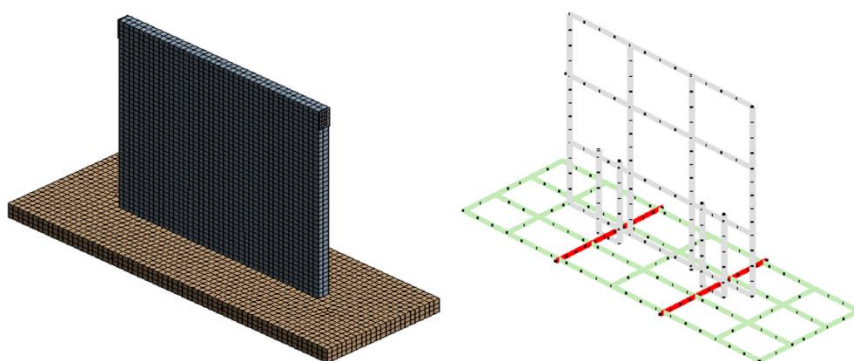


Fig. 3 Mesh of Raft and wall

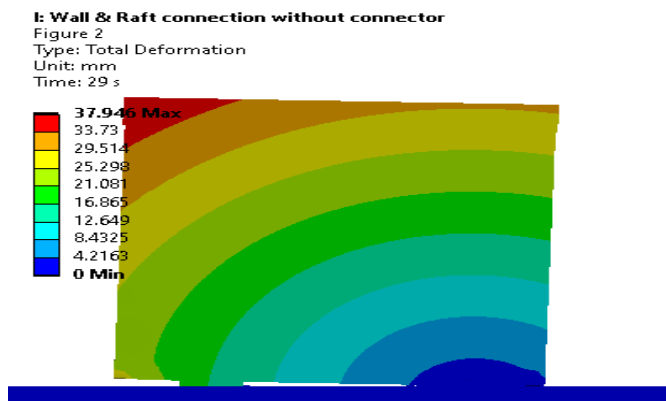


Fig. 4 Deflection for the wall without connector

3. Experimental Investigation on The Precast Specimen

3.1 Properties of Materials Used For Casting of Precast Specimen

Materials are all in compliance with Indian standards. Portland Pozzolana Cement(PPC), per IS 1489 (part 1): 1991, was the cement used in the specimens [33]. The coarse and fine aggregate utilized in the mix design satisfies Zone-III requirements in IS 383-1970 [34] and has a fineness modulus 2.34. The study used two kinds of crushed coarse aggregates, one with a nominal size of 20 mm and a specific gravity of 2.62. Tables 4-8 provide information on the characteristics of several materials utilized in the experiment.

Table 4. Physical characteristics of PPC

Characteristics	Obtained values	Value as per IS:1489 (Part 1) – 1991
Standard Consistency(%)	31	
Fineness Of Cement	0.78	≥ 10%
Setting Time Initial	43 min	≤30 min
Setting Time Final	285 min	≥ 600 min
7 days Compressive Strength (MPa)	24.5	≤ 22.0
28 days Compressive Strength (MPa)	35.5	≤ 33.0

Table 5. Physical characteristics of coarse aggregate

Characteristics	Values
Form	crushed
Max.Nominal size (mm)	20
Specific Gravity	2.65
Water Absorption (%)	2.03
Fineness Modulus	6.79

Table 6. Physical characteristics of fine aggregate

Characteristics	Values
Specific Gravity	2.7
Bulk Modulus (kg/l)	1.35
Fineness Modulus	2.28
Water Absorption (%)	2.40
Grading zone as per IS: 383–1970	III

Table 7. Properties of rebars

Size	Yield Strength(N/mm ²)	Ultimate Strength(N/mm ²)	Elongation (%)
8mm	554.65	670.69	20.53
10mm	557.26	676.84	25.81
12mm	561.32	702.71	31.25

Table 8. M20 mix design

Materials	Quantity(kg)
Cement	396.62
Fine Aggregates	572.69
Coarse Aggregates	1172.86
Water	189.91

3.2 Description of precast specimens

Table 9 shows the five raft-wall connections used in this study's experimental study: RW1, RW2, RW3, RW4, RW5, and RW6. Two of these specimens are made from standard individuals with no connections. The other two are made from 8 mm and 10 mm shear

connectors, and the final two specimens are made with 12mm rods as shear connectors. The shear connections are used to ensure the joint’s shearing capability. The components of the wall-raft specimens were designed and detailed per IS 456-2021. To reinforce all specimens longitudinally and transversally, high-yield strength Fe-550 steel bars were used. As indicated in Table 7, the longitudinal steel’s yield and ultimate strengths were 554.65 and 670.69 for 8 mm, 557.26 N/mm² and 676.84 N/mm² for 10 mm diameter rods, and 561.32 and 702.71 for 12mm. The only difference between the 5 specimens is the diameter of the shear connector rods. Figures 5 and 6 show schematics of the longitudinal and transverse reinforcing details for the 6 specimens' walls and rafts. The cross-section chosen is 77 x 1000 mm for the entire wall, with a height of 1000 mm. The concrete connector’s dimensions are 100 x 50 mm and 110 x 560 mm for the raft, for a total length of 1600 mm. Figure 7 represents the overall reinforcements of the precast wall and raft specimen. Specimens RW3, RW4, and RW5 are connected to the raft without grouting using 8mm, 10mm, and 12mm rods as shear connectors. RW6 is also connected to a raft without grouting with a 12 mm rod shear connector for earthquake loading.

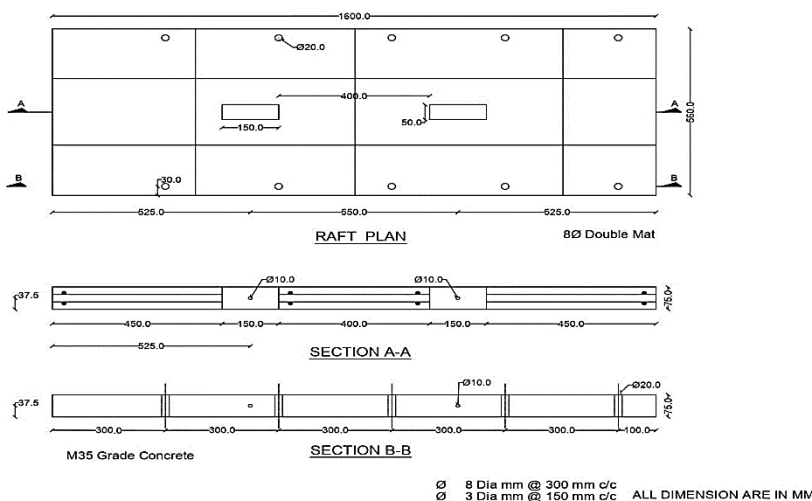


Fig. 5 Schematic representation of raft

Table 9. Casted specimens

Specimen	Representation
RW1	Wall raft without connector and no grouting
RW2	Wall raft without connector and with grouting
RW3	Wall-raft with shear connector 8mm
RW4	Wall-raft with shear connector 10mm
RW5	Wall-raft with shear connector 12mm
RW6	Wall-raft with shear connector 12mm and earthquake loading

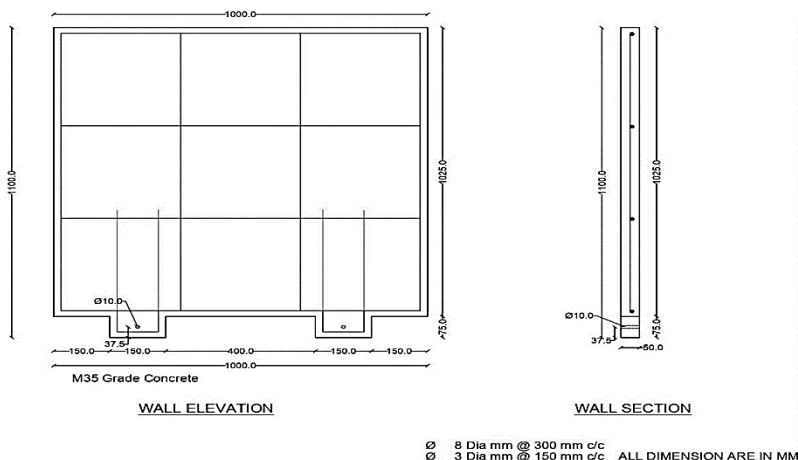


Fig. 6 Schematic representation of the wall

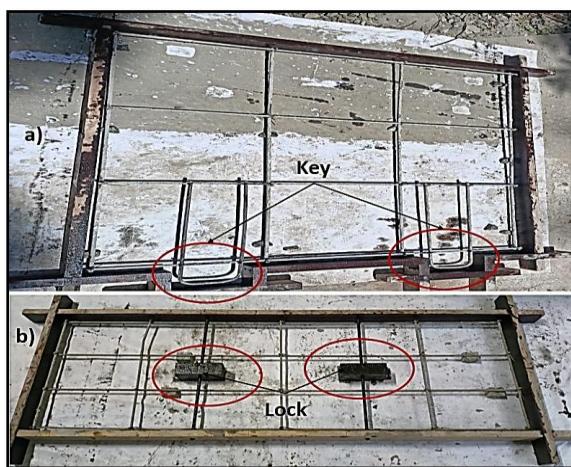


Fig. 7 Reinforcement detailing for a) wall, b) raft

3.3 Setup for the Experimental Investigation

The experimental work aims to examine the wall and raft connection behaviour under lateral loading by implementing cyclic load tests. An experimental arrangement was established to achieve this objective, consisting of loading devices, base fixtures, lateral supports, and instrumentation. Figure 8 shows a schematic of the loading test configuration used on the Raft-wall connection. The raft is mounted horizontally and is held in place by a fixed support.

Figure 9 depicts the instrumentation that included a data-collecting system utilised to observe the load-deformation behaviour. However, applying axial loads on the columns was not feasible in this study due to limitations in the available testing equipment and challenges associated with real-time force control. The experimental setup employed in this investigation is elucidated in the subsequent section.



Fig. 8 Experimental setup of the raft and wall connection

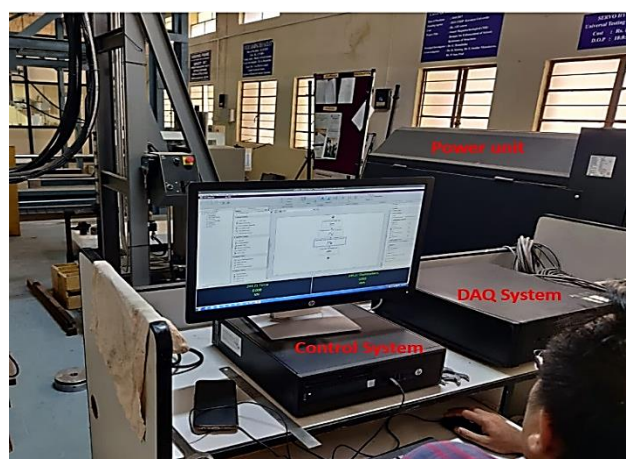


Fig. 9 Control system with DAQ

The experiment is being conducted at the Department of Civil Engineering's structural Engineering lab at the Karunya Institute of Technology and Sciences in Coimbatore, India. A servo-hydraulic system controls the actuator that is employed in the experiment. The actuator has a maximum stroke length of 125 mm in both directions and a capacity of 500kN (in tension and compression). The load cell and displacement transducer previously integrated inside the actuator made measuring the force and displacement produced by the actuator's piston easier.

On the other hand, the transverse wall is oriented vertically, and the wall tip is maintained in place by the actuator. This study's test methodology is similar to that utilized by Roy et al. [35], Park and Paulay [36], and Hakuto et al. [37] and differs where no axial force was applied to the raft throughout the testing. Each specimen is subjected to cyclical loading based on displacement. Figure 3 illustrates the control system and the DAQ system for data collection. ACI 374 states that for each level of increasing deformation, the number of cycles required to create damage equal to the number of cycles at a specific drift level must be doubled by at least two, and thus the applied displacement was repeated for 2 cycles throughout the experiment. The displacement was steadily increased during this study to obtain realistic inter-story drift-ratio of 0.5 percent, 0.7 percent, 1.0 percent, 1.5 percent, 2.0 percent, 3 percent, 4 percent, 5 percent, 6 percent, and 7 percent. Figure 10 shows the

displacement histories that were applied to all of the specimens similar to the loading pattern of Ebanesar et.al.[38].

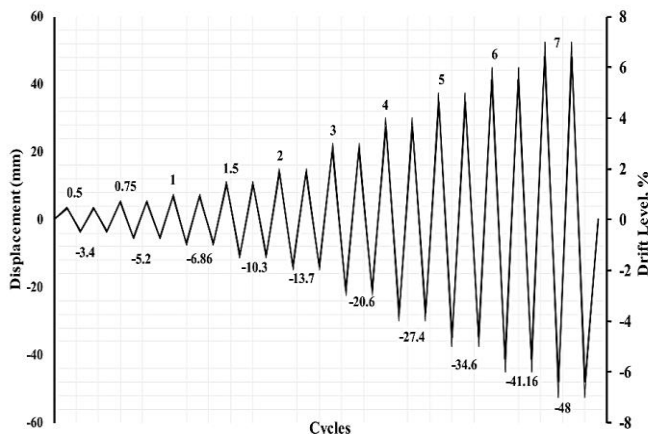


Fig. 10 Cyclic loading pattern for experimental purpose

3.4 Observation During The Experimental Investigation

While experimenting, some interesting observations concerning the various RW specimens emerged. The first cracks appeared at the key and lock interface of specimen RW1 at a drift-ratio of 0.7% (0.57 kN) of the third forward cycle. With increased loading, shear cracks are developed mainly in the key of the wall. No flexural cracks were observed on the RW joining faces during the experiment. The shearing in the joint and the raft caused degradation of the key in the specimen leading to failure. In the forward and reverse directions, the maximum lateral load was 1.22 kN and 2.27 kN, respectively.



Fig. 11 Observation from RW1 specimen



Fig. 12 Failure from RW1 specimen

The wall uplift can be seen in Figure 11, which was created because no grouting or connectors were used. This one exhibited significantly less restraint on its uplift movement than other specimens. It is observed that the wall is uplifted back and forth. The RW1 specimen experiences complete failure at the key, which was used for connection to the

raft footing. This failure occurs as the displacement increases. It was observed that the key had been completely distorted, as shown in Figure 12.



Fig. 13 Observation from RW2 specimen

Grouting is done in the gap between the wall panel and raft. The area grouted has been circled and presented in Fig 13 . As a high-strength, non-shrink, cementitious precision grout, Fosroc Conbextra GP2 is used as grouting material. In numerous industries, including construction and civil engineering, it is frequently employed for precise grouting and anchoring applications. Conbextra GP2 is renowned for its superior flow characteristics, high early and ultimate strengths, and chemical resistance.

For grouted specimen RW2, Cracks were observed all over the connecting face of the wall and the raft footing, which is depicted in Figure 13, which also shows the initial crack pattern. Because the damage was confined to the grouting mortar only, the specimen did not appear to have suffered any significant losses. The first cracks appeared in specimen RW1 during the first cycle, with drift-ratio of 0.7% (0.65kN) in the grouted area. With increased loading, these cracks spread throughout the grouted region. Under the applied load, there is a lack of confinement, and thus the shear cracks are visible in the key and lock region, causing structural deformation. The specimen's shear failure was caused by decreasing concrete strength in the joint core of the lock and key. The maximum lateral load in the forward and reverse directions was 1.72 kN and 3.95 kN, respectively.

The observations made by RW3, RW4, RW5, and RW6 were entirely dissimilar to those made by RW1 and RW2. For the specimens RW3, RW4, RW5, and RW6, where connectors were used, the connector rod restricted the rocking movement as the displacement increased. In general, for specimens RW3, RW4, RW5, and RW6, hairline shear cracks were formed perpendicular to the key and lock joint region. The formation of shear cracks form whenever there is an increase in displacement, as shown in Figure 14. Figure 15 illustrates the initial failure of joints in the wall's key area and the raft footing's lock area. This phenomenon was observed for specimens that contained connector rods. It has been found that the initial shear cracks are always accompanied by the initial failure at the joints of the wall and the raft, which is later followed by the complete failure of the specimen, as shown in Figure 16.



Fig. 14 Shear crack from the specimen with connector



Fig. 15 Initial failure of RW joints with connector



Fig. 16 Complete failure of RW joints with connector

Shear cracks were produced at 2% drift-ratio for RW3 at a displacement of 13.69mm (forward first cycle). Hairline shear cracks were discovered in the raft footing face perpendicular to the joint region. The pinching length steadily rose until it reached a drift-ratio of 4%. Further cracks formed after the 5% DR and substantial damage was noticed in the joint area. After 5% drift, the raft wall interface widened, and concrete failure mode developed within the joint area. This specimen's maximum lateral load was 4.98 kN in the forward direction and 5.96 kN in the reverse direction. The specimen failed due to degeneration of the joint core, which was caused by deterioration of the lock-key joint region. For specimen RW4, under a load of 6.35 kN (3.5% drift-ratio), the first shear crack manifested itself in the third forward cycle. After increasing the load, cracks in the RW interface joint were found. Hairline shear cracks were seen on the face of the raft footing perpendicular to the joint region at a drift level of 3.5% (reversed first cycle) and a displacement of 20.78 mm. At the lock-key interface, the cracks widened at the same drift-ratio. A progressive increase followed the DR of 3.5% in the pinching length. After a drift-ratio of 4%, new cracks in the lock-key joint area appeared. After 5% drift-ratio, the RW joint interface damage grew severely. This specimen could withstand a lateral force of up to 8.17 kN going forward and 8.04 kN backwards.

Ultimately, the specimen failed because the lock-key joint region of the concrete had failed. The initial shear crack appeared in the fourth forward cycle of specimen RW5 with a load of 7.59 kN (4.5% drift-ratio). Cracks in the RW joint contact were discovered after increasing the tension. At a drift-ratio of 4.5% (reversed fourth cycle) and a displacement of 26.88 mm, the raft footing face perpendicular joint region revealed hairline diagonal cracks. With the same drift-ratio, the fissures grew at the lock-key interface. A steady rise in pinching length after 4.5% drift-ratio. Severe cracks in the lock-key joint area were discovered after a 5% drift-ratio.

The RW joint interface damage increased significantly after 5% drift-ratio. This specimen could bear lateral forces of up to 9.82 kN in the forward direction and 10.23 kN in the reverse direction. Finally, the specimen failed because the concrete's lock-key joint region collapsed. To better understand the RW behaviour, specimen RW6 was subjected to data from the El Centro earthquake. During the process of installing the system, the time-history data for El-Centro was supplied by the MTS corporation. The specimen achieved a maximum load of 3.65 kN when moving in a forward direction and 6.36 kN when moving in a backward direction. The maximum displacement that the specimen goes through is 9.27 mm in the forward direction and 12.92 mm in the reversed direction. It was found that the lock-key interface region had sustained considerable damage comparable to the damage sustained by the earlier specimens that contained the connector rod.

Under the experimental results, using steel rods as shear connectors in RW joints significantly increased the load-deflection behaviour. All specimens outperform the control specimens in RW1 and RW2. The specimens RW1 and RW2 fail with complete deterioration of the key but minor damage to the lock region. In contrast, the specimens with steel rods of any diameter as shear connectors fail with initial shear cracks perpendicular to the key-lock joint on the face of the raft footing and complete failure due to severe deterioration of both the key-lock and the region around the joints. Two significant findings were observed: (a) a delay in key-lock joint deterioration in specimens with connector rods compared to specimens without connectors. (b) When the diameter of the connector rod is increased, shear fracture formation is delayed, resulting in the complete deterioration of the lock-key joint. Figure 16 depicts the generalized failure of the specimens RW3, RW4, RW5, and RW6. More micro fractures are found in these specimens in the early stage as the drift-ratio increases by 3.5%. The cracks in the RW joint interface become severe and waste more energy.

4. Results and Discussion

Figure 17-Figure 21 compares the performance of RW joints in terms of force-displacement curves and the hysteresis curves acquired from experimental observations and FEA analysis for all specimens. It is evident from the hysteresis plots that the experimental and FEA models agree with each other with an error lesser than 10%, which is acceptable in comparison [4-6][13][24]. The values obtained from the FEA model are presented in the table for comparison purposes. This strengthening technique improves the ultimate load-carrying capacity of RW with shear connectors strengthened specimens over reference specimens while also lowering shear demand. RW5 was found to yield the maximum performance. The maximum load-carrying capacity of the strengthened RW5 specimen was 9.82 kN in the forward direction and 10.23 kN in the reversed direction. It is inferred from Figure 9 that after a displacement of 42mm in the opposite direction, the load begins to fall. It is possible to conclude that lock-key joint failure occurs later in strengthened specimens than in specimens without connectors.

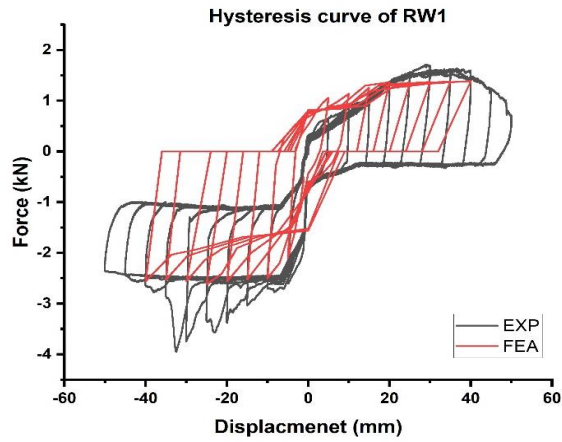


Fig. 17 Hysteresis plot for RW1(no connector)

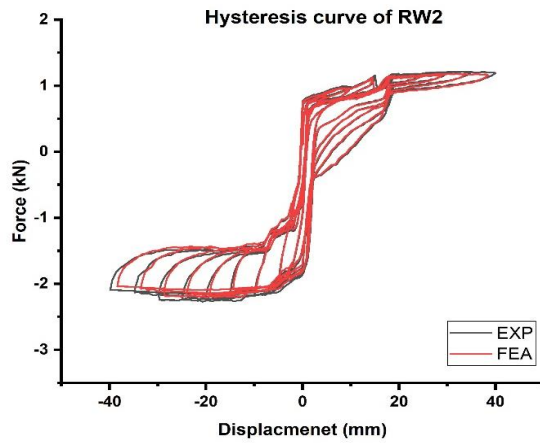


Fig. 18 Hysteresis plot for RW2(with Grouting)

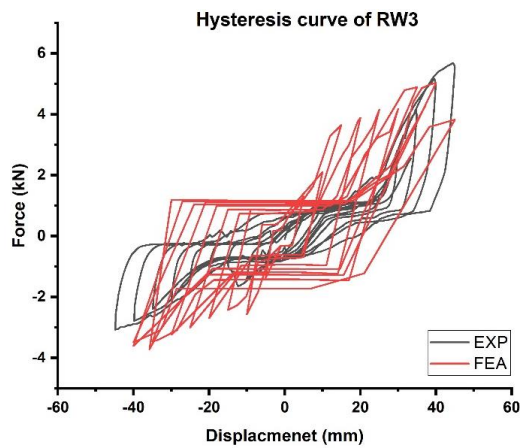


Fig. 19 Hysteresis plot for RW3(8mm connector)

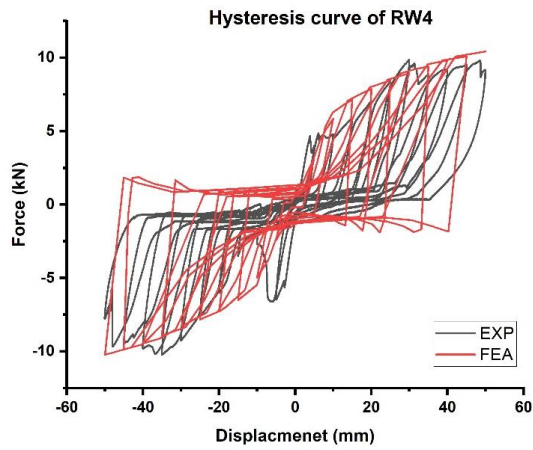


Fig. 20 Hysteresis plot for RW4(10mm connector)

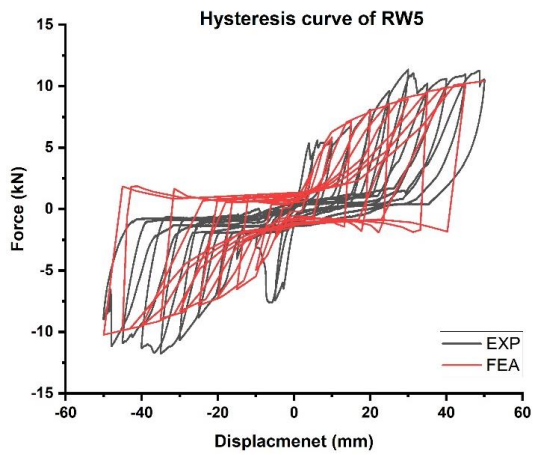


Fig. 21 Hysteresis plot for RW5(12mm connector)

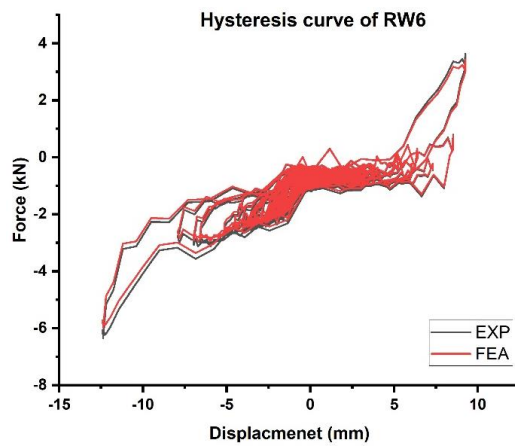


Fig. 22: Hysteresis plot for RW6(12mm connectors)

The grouted specimen RW2 and specimens with steel rod connectors, RW3, RW4, RW5, and RW6, have a load-carrying capacity increase of 39.32%, 67.42%, 78.77%, 82.84%, and 65.63% over the specimens without grouting or any connector rods (RW1). According to the test results, adding steel rods as shear connector reinforcement significantly increases the load-bearing ability. Therefore, shear connectors in RW joint-strengthened specimens would suit RC constructions in seismically active regions. The results from the study discussed above have been tabulated in Table 10 for a clear view of the change in the load-carrying capacity of the RW under cyclic loading.

Table 10. Capacity for lateral loads

Spec.	Initial Shear crack (kN)	Initial Shear crack disp. (mm)	Experimental Model		FEA Model		Percentage Variation	
			Max load+ve (kN)	Max load-ve (kN)	Max load+ve (kN)	Max load-ve (kN)	Max load+ve (%)	Max load-ve (%)
RW1	0.52	5.23	1.22	2.27	1.19	2.15	2.45	5.28
RW2	0.96	8.36	1.72	3.95	1.68	3.88	2.32	1.77
RW3	1.24	13.69	4.98	5.66	4.55	5.21	8.63	7.93
RW4	1.58	20.78	8.17	8.04	8.25	8.12	0.96	0.98
RW5	1.63	26.88	9.82	10.23	9.98	10.63	1.60	3.76
RW6	1.91	12.92	3.65	6.36	3.55	6.45	2.73	1.39

The energy dissipation capability of a structure is a crucial factor to consider when assessing how well it performs when subjected to seismic excitations. The utilisation of transverse shear reinforcement as a shear connector resulted in a notable increase in the peak load-carrying capacity of the specimen. This increase was directly proportional to the more excellent energy dissipation exhibited by the specimen [39]. Consequently, energy dissipation without a considerable loss of stiffness or strength indicates the structure's capability. A structure can release more energy by supplying enough inelastic deformation in a key area or enough ductility in its connections. The energy dissipation capacity is defined as the region under the hysteresis loop for each load cycle.

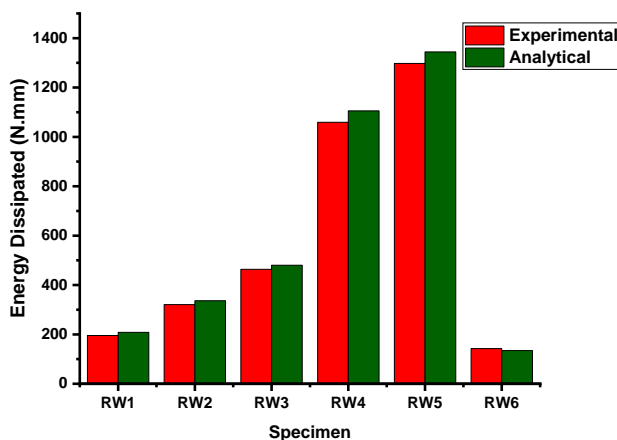


Fig. 23 Energy dissipation plot

Cumulative energy dissipation may be computed by adding the load-displacement loop throughout the test. Fig. 23 shows the usual cumulative energy determined from the area under the force-displacement curves of test specimens. The following equation was used to calculate how hysteretic energy dissipation was standardized to the area of an elastic perfectly-plastic rectangular block at each load cycle [40,41]:

$ED = \frac{A}{4 \cdot V_{max} \cdot \delta_{max}}$ or normalized ED. A = region encircled by the hysteresis loops, V_{max} = maximum load, and δ_{max} = maximum displacement in positive and negative directions during the ultimate cycle.

Maximum ED observed from the experimental and FEA model findings is tabulated in Table 11 for a clear understating.

Table 11. Energy dissipated by the specimens

Specimen	Energy Dissipation (N-mm)		Percentage Variation (%)
	Experimental	FEA Model	
RW1	195.41	208.43	6.24
RW2	320.65	336.29	4.65
RW3	463.78	480.23	3.42
RW4	1059.23	1105.64	4.19
RW5	1297.48	1344.43	3.49
RW6	142.49	134.28	5.76

It can be inferred that with an increment in the diameter of the steel rod connector, the energy dissipating capacity of the raft wall connection increases and, thus, resistance to seismic forces.

5. Conclusions

The present study examines the precast reinforced concrete walls using the grouting technique and steel rods as shear connectors subjected to cyclic loading conditions. A total of six RW joint specimens were developed following the stipulations outlined in Indian codal provisions (IS 456:2021). The specimens subjected to cyclic loadings were equipped with grouting and shear connectors. The testing parameters of the study encompass load-carrying capacity, hysteresis responses, and crack patterns. The analysis conducted in this study yielded the subsequent conclusions:

- The hysteresis behaviour and energy dissipation capacity of the Finite Element Analysis (FEA) model are verified through experimental validation with a variation of less than 10%.
- The Finite Element Analysis (FEA) and experimental testing findings demonstrate a direct correlation between the addition of shear connector rod diameter and the corresponding enhancement in load-carrying capacity.
- The load-carrying capacity of the specimen utilising a 12mm steel rod as a shear connector (RW5) exhibited a maximum increase of 82.84% when compared to the standard specimen. The reinforced specimens (RW2, RW3, RW4, and RW6) exhibited notable performance improvements, with gains of 39.32%, 67.42%, 78.77%, and 65.93%, respectively.
- In the specimens where shear connectors were employed, shear cracks were observed perpendicular to the wall key. An increase in shear connectors' diameter leads to a reduction in the width of shear cracks. Typically, the failure of specimens featuring shear connectors can be ascribed to the degradation of the wall key inserted within the raft footing.

- In conclusion, the steel rod connector proposed for the RW joint presents an alternative configuration that exhibits improved performance when subjected to cyclic and seismic loads. Moreover, the proposed utilisation of steel rods as shear connections represents an innovative approach to enhance the structural integrity of the existing RW precast connection. Furthermore, when comparing the specimen utilising a steel rod as a shear connection to the reference specimen, it is observed that the former exhibits a relatively less substantial level of damage.
- The results obtained from this study can be utilised as a foundation for subsequent verification and enhancement of the suggested method for strengthening. Future research may consider conducting theoretical approaches to validate the obtained results and evaluate the performance of the RW joint under different loading conditions. To ascertain the sustained efficacy of the proposed reinforcement method, it is imperative to conduct a comprehensive assessment of its long-term durability. Subsequent investigations could potentially prioritise evaluating the durability of the grouting material and shear connectors concerning various environmental influences, including moisture, corrosion, and ageing. This would be done to guarantee the long-term effectiveness of the RW joint when implemented in practical scenarios.

Acknowledgement

The authors acknowledge that Structural Dynamics Laboratory supports this study in the Karunya Institute of Technology and Sciences.

References

- [1] Arthi S, Jaya KP. Experimental study on shear behaviour of precast shear wall-slab dowel connection. *Asian J Civ Eng.* 2020;21(4):663-76. <https://doi.org/10.1007/s42107-020-00229-z>
- [2] Arthi S, Jaya KP. Hysteresis behaviour of precast shear wall-slab connection under reverse cyclic loading. In: *IOP Conference Series. IOP Conf Ser.: Mater Sci Eng* (Vol. 936, No. 1, p. 012039). 2020, September;936(1). <https://doi.org/10.1088/1757-899X/936/1/012039>
- [3] Arthi S, Jaya KP. Seismic performance of precast shear wall-diaphragm connection: a comparative study with monolithic connection. *Int J Civ Eng.* 2020;18(1):9-17. <https://doi.org/10.1007/s40999-019-00444-z>
- [4] Soleimani-Abiat MR, Banan M. Seismic behavior of RC building by considering a model for shear wall-floor slab connections. *Comput Concr.* 2015;16(3):381-97. <https://doi.org/10.12989/cac.2015.16.3.381>
- [5] Brunesi E, Nascimbene R. Experimental and numerical investigation of the seismic response of precast wall connections. *Bull Earthquake Eng.* 2017;15(12):5511-50. <https://doi.org/10.1007/s10518-017-0166-y>
- [6] Brunesi E, Peloso S, Pinho R, Nascimbene R. Cyclic testing of a full-scale two-storey reinforced precast concrete wall-slab-wall structure. *Bull Earthquake Eng.* 2018;16(11):5309-39. <https://doi.org/10.1007/s10518-018-0359-z>
- [7] Brunesi E, Peloso S, Pinho R, Nascimbene R. Cyclic tensile testing of a three-way panel connection for precast wall-slab-wall structures. *Struct Concr.* 2019;20(4):1307-15. <https://doi.org/10.1002/suco.201800280>
- [8] Brunesi E, Peloso S, Pinho R, Nascimbene R. Shake-table testing of a full-scale two-story precast wall-slab-wall structure. *Earthquake Spectra.* 2019;35(4):1583-609. <https://doi.org/10.1193/072518EQS184M>

- [9] Chalot A, Roy N, Michel L, Ferrier E. Mechanical behavior of a full-scale RC wall-slab connection reinforced with frp under cyclic loading. *Eng Struct.* 2021;239:112146. <https://doi.org/10.1016/j.engstruct.2021.112146>
- [10] Devine F, Olund O, Elwood K, Adebar P. Seismic performance of concrete tilt-up buildings: current wall-to-slab connections. In: *Proceedings of the 14th. Beijing, China: World Concrete on Earthquake Engineering*; 2008. p. 12-7.
- [11] Guo W, Zhai Z, Cui Y, Yu Z, Wu X. Seismic performance assessment of low-rise precast wall panel structure with bolt connections. *Eng Struct.* 2019;181:562-78. <https://doi.org/10.1016/j.engstruct.2018.12.060>
- [12] Hamicha A, Kenea G. Investigation on the effect of geometric parameter on reinforced concrete exterior shear wall-slab connection using finite element analysis. *Adv Civ Eng.* 2022;2022:1-17. <https://doi.org/10.1155/2022/4903650>
- [13] Hemamalini S, Vidjeapriya R, Jaya KP. Performance of precast shear wall connections under monotonic and cyclic loading: A state-of-the-art review. *Iran J Sci Technol Trans Civ Eng.* 2021;45(3):1307-28. <https://doi.org/10.1007/s40996-020-00530-6>
- [14] Henry RS, Ingham JM, Sritharan S. Wall-to-floor interaction in concrete buildings with rocking wall systems. In: *Proceedings of the NZSEE Annual Conference. Christchurch, New Zealand*; 2012, April.
- [15] Krentowski JR, Knyziak P, Mackiewicz M. Durability of interlayer connections in external walls in precast residential buildings. *Eng Fail Anal.* 2021;121:105059. <https://doi.org/10.1016/j.engfailanal.2020.105059>
- [16] Lu Y, Chen W, Xiong F, Yan H, Ge Q, Zhao F. Seismic performance of a full-scale two-story bolt-connected precast concrete composite wall panel building tested on a shake table. *J Struct Eng.* 2021;147(12):04021209. [https://doi.org/10.1061/\(ASCE\)ST.1943-541X.0003183](https://doi.org/10.1061/(ASCE)ST.1943-541X.0003183)
- [17] Pavel F, Vacareanu R, Marcu D. Seismic performance assessment and rating for a flat-slab RC core wall structure in Bucharest, Romania. *Structures.* 2021, June;31. <https://doi.org/10.1016/j.istruc.2021.02.036>
- [18] Pavese A, Bournas DA. Experimental assessment of the seismic performance of a prefabricated concrete structural wall system. *Eng Struct.* 2011;33(6):2049-62. <https://doi.org/10.1016/j.engstruct.2011.02.043>
- [19] Rossley N, Aziz FNAA, Chew HC. Behaviour of precast walls connection subjected to shear load. *J Eng Sci Technol.* 2014;10:142-50.
- [20] Shen SD, Cui Y, Pan P, Gong RH, Miao QS, Li WF. Experimental study of RC prefabricated shear walls with shear keys affected by a slotted floor slab. *J Aerosp Eng.* 2019;32(3):04019013. [https://doi.org/10.1061/\(ASCE\)AS.1943-5525.0001000](https://doi.org/10.1061/(ASCE)AS.1943-5525.0001000)
- [21] Shen Y, Ni Z, Ai T, Dai M, Jiang B. Experimental study on postfire behavior of a novel assembled wall-slab joint. *Adv Struct Eng.* 2023;26(6):1142-58. <https://doi.org/10.1177/13694332231153939>
- [22] Singhal S, Chourasia A. Joint connections for precast structural concrete components. In: *16th Symposium on Earthquake Engineering*; 2018, December.
- [23] Singhal S, Chourasia A. Seismic resistance of precast reinforced concrete shear wall: experimental and analytical study. In: *Proceedings of the 8th int engineering symp. Kumamoto, Japan. Kumamoto University*; 2019, March.
- [24] Singhal S, Chourasia A, Chellappa S, Parashar J. Precast reinforced concrete shear walls: state of the art review. *Struct Concr.* 2019;20(3):886-98. <https://doi.org/10.1002/suco.201800129>
- [25] Singhal S, Chourasia A, Kajale Y, Singh D. Behaviour of precast reinforced concrete structural wall systems subjected to in-plane lateral loading. *Eng Struct.* 2021;241:112474. <https://doi.org/10.1016/j.engstruct.2021.112474>
- [26] Singhal S, Chourasia A, Panigrahi SK, Kajale Y. Seismic response of precast reinforced concrete wall subjected to cyclic in-plane and constant out-of-plane loading. *Front Struct Civ Eng.* 2021;15(5):1128-43. <https://doi.org/10.1007/s11709-021-0753-5>

- [27] Tatsambon L, Massé N, Hervé-Secourgeon E, Hervé-Secourgeon G, Théodore CÉ. Impact of a hybrid modelling for wall/wall and wall/slab connections on the constructability of reinforced concrete nuclear building; 2022.
- [28] Vaghei R, Hejazi F, Firoozi AA, Jaafar MS. Performance of loop connection in precast concrete walls subjected to lateral loads. *Int J Civ Eng.* 2019;17(3):397-426. <https://doi.org/10.1007/s40999-018-0366-0>
- [29] Vaghei R, Hejazi F, Taheri H, Jaafar MS, Ali AAA. A new precast wall connection subjected to monotonic loading. *Comput Concr.* 2016;17(1):1-27. <https://doi.org/10.12989/cac.2016.17.1.001>
- [30] Wang J, Kusunoki K. Study on the flexural strength of interior thick wall-thick slab joints subjected to lateral force using finite-element analysis. *Buildings.* 2022;12(5):535. <https://doi.org/10.3390/buildings12050535>
- [31] Xia K, Hu X, Xue W. Experimental studies on in-plane connections of composite beam-precast concrete shear wall under reversed cyclic loading. *Structures.* 2021, December;34. <https://doi.org/10.1016/j.istruc.2021.08.127>
- [32] Zenunović D, Folić R. Models for behaviour analysis of monolithic wall and precast or monolithic floor slab connections. *Eng Struct.* 2012;40:466-78. <https://doi.org/10.1016/j.engstruct.2012.03.007>
- [33] IS: 1489 (Part 1)-1991. Portland-Pozzolana Cement specification Part 1, Fly ash based. New Delhi: Bureau of Indian Standards.
- [34] IS: 383-1970. Specification for coarse and fine aggregates from natural sources concrete. New Delhi: Bureau of Indian Standards.
- [35] Park R, Paulay T. Reinforced concrete structures. New York: John Wiley & Sons; 1975. <https://doi.org/10.1002/9780470172834>
- [36] Hakuto S, Park R, Tanaka H. Retrofitting of reinforced concrete moment resisting frame. *Res Reprod.* 1995;95-4:1.
- [37] Roy B, Laskar AI. Cyclic behavior of in-situ exterior beam- column subassemblies with cold joint in column. *Eng Struct.* 2017;132:822-33. <https://doi.org/10.1016/j.engstruct.2016.12.001>
- [38] Ebanesar A, Gladston H, Farsangi EN, Sharma SV. Strengthening of RC beam-column joints using steel plate with shear connectors: Experimental investigation. *Structures* 2022; 35: 1138-1150. <https://doi.org/10.1016/j.istruc.2021.08.042>
- [39] Rath, B., Garoma, S., Kudama, R. et al. Effect of different width ratio and transversal link pattern on the load carrying capacity of partially encased composite column. *Asian J Civ Eng.* 2023; 24: 205-218. <https://doi.org/10.1007/s42107-022-00498-w>
- [40] Shannag MJ, Abu-Dyya N, Abu-Farsakh G. Lateral load response of high performance fiber reinforced concrete beam-column joints. *Constr Build Mater.* 2005;19(7):500-8. <https://doi.org/10.1016/j.conbuildmat.2005.01.007>
- [41] Siva Chidambaram R, Agarwal P. Seismic behavior of hybrid fiber reinforced cementitious composite beam-column joints. *Mater Des.* 2015;86:771-81. <https://doi.org/10.1016/j.matdes.2015.07.164>